Energy Proceedings
Vol 31, 2023
ISSN 2004-2965

Charge Transfer Mechanism for Plasmon-Mediated Photocatalytic Water Splitting On Gold Clusters

Qingying Feng[1,2], Ying Zhang[1,2], Dong Liu[1*], Qiang Li[1*]

1 School of Energy and Power Engineering, Nanjing University of Science and Technology, Nanjing 210094, China

2 These authors contributed equally

(*Corresponding Author)

ABSTRACT

Plasmonic photocatalysts provide means to efficient solar water splitting. Recently, researchers proposed that high-energy hot carriers generated by plasmon resonance can be transferred directly to the adsorbates, driving photochemistry, which differs from the previous indirect charge transfer forming electron-hole pairs. This study analysed underlying mechanism of charge transition channel in plasmon-driven photochemistry at the atomic scale, and evidence was provided for distinguishing between different modes of charge transfer. A specific example, where a cluster of six gold atoms interacts with one water molecule, was investigated. Based on combined density functional theory (DFT), Linear-Response time-dependent density functional (LR-TDDFT) and Ehrenfest dynamics simulations, the results revealed that hot electrons selectively transfer to high-energy unoccupied orbitals through indirect single-particle excitations or direct plasmon decay excitations. Direct transition was more conducive to photochemical reactions due to its higher energy.

Keywords: Surface plasmon resonance; Time-dependent density functional theory; Charge transfer; Au cluster

NONMENCLATURE

Abbreviations	
LR-TDDFT	Linear-Response Time-dependent Density Functional
LSPR	Localized Surface Plasmon Resonance
K-S	Kohn–Sham
Symbols	
E	Electric field
ω	Frequency
τ	Width of laser pulse

1. INTRODUCTION

With the widespread interest in photocatalysis for the direct conversion of solar energy into chemical energy, the development of highly efficient photocatalysts capable of a wide range of solar radiation absorbance has become essential. Plasmon nanoparticles can efficiently capture visible light and excite localized surface plasmon resonance (LSPR).[1-3] In conventional industry, the thermal effect of metal particles is used for reactions such as oxidation and ammonia synthesis, requiring very high temperatures.[4] In addition, carrier-driven photochemistry requires external light fields with very high intensities to excite electron-hole pairs.[5] However, plasmon-driven photocatalysis can effectively overcome these limitations, and experiments have demonstrated that metal nanoparticles can conduct chemical reactions at much lower light intensities and temperatures.[6] Under light irradiation, the incident electromagnetic radiation interacts with free electrons of the metal nanoparticles and generates plasmon resonance closing to the particle surface. The energy of LSPR excitation then can be dissipated either by emitting photon radiation or generating high-energy carriers within the

nanoparticles.[7-9] These high-energy carriers then directly drive photochemical reactions on the surface of nanoparticles[10, 11].

LSPR-induced chemical reaction differs from thermal excitation and allows for efficient conversion of solar energy to chemical energy. However, the mechanism of plasmon-induced photocatalysis is unclear, mainly because of the difficulty in observing ultrafast processes. So far, direct charge transfer and indirect charge transfer are the most discussed major microscopic mechanisms to explain the chemical reactions promoted by plasmon excitations[12-14]. It is also proposed that relaxation of hot carriers can lead to the local thermal effect which could activate the reaction[15]. Since there is no universally accepted explanation, many studies gave their own interpretation of the mechanism[13, 16-18]. Despite the challenges of experiment, Wu et al.[14] demonstrated that a plasmon could decay by exciting an electron from the metal to an acceptor directly with strongly coupling through ultrafast transient absorption studies in metal-to-semiconductor system. Boerigter et al.[10] measured anti-Stokes and Stokes surface-enhanced Raman scattering intensities to explain temperature difference between nanoparticles and adsorbed molecules, inferred high rates of direct, resonant flow of charge between metal and adsorbate bypassing the conventional charge excitation and thermalization process. Although these studies provided evidence of macroscopic charge transfer pathways in an experimental perspective, interpreting transfer pathways from a micro perspective still to be challenging.

Since the ultrafast dynamics of chemical reactions is somewhat difficult to be probed, theoretical calculation becomes an essential approach to investigating plasmon excitations. Early researches of plasmon studied by Beck et al.[19-20] used jellium sphere models in Linear-Response TDDFT. However, it was not possible to distinguish between single-particle excitations and plasmon oscillations because of the coupling in this model. Recently, a method for distinguishing the two modes of excitations using Real-Time TDDFT Ehrenfest dynamics simulations was proposed by Ma et al.[21] Real-Time TDDFT considers time-dependent Hamiltonian quantities to describe time evolution of the ground state Kohn−Sham system, which is the reason for its popularity in recent years.[22-23] So far most of the studies were only carried out on the hydrogen dissociation, which is a relatively simple model in plasmon excitation.[2, 24] More complex processes deserve to be explored.

In this work, atomic details of water splitting catalyzed by plasmon metal nanoparticles were demonstrated. Charge transfer pathways were distinguished in detail from an atomic perspective.

2. CALCULATION METHODS

2.1 General setups of first-principles calculations

The system studied in this work is a cluster comprising six gold atoms (Au6) with one water molecule adsorbed on the tip as shown in Fig. 1a. The energy favorable feature of this system has been supported by mobility measurements of charged gold clusters[29]. All first-principles density functional theory (DFT) calculations in this work were performed using the OCTOPUS code, a GNU Public Licensed software package[25-26]. Local density approximation functional was employed for all calculations. A sphere with a radius of 6 angstroms at the centre of each atom was taken as simulation box. And the spacing between the real-space grid points was set to 0.4 a.u. Systematic structure and K-S orbital wave functions were visualized using VMD[27]. The $5d^{10}6s^{1}$ electrons of the gold atoms, $2s^{2}2p^{4}$ electrons of the oxygen atoms and $1s^{1}$ electrons of the hydrogen atoms were treated as valence electrons using Norm-conserving pseudopotential[28].

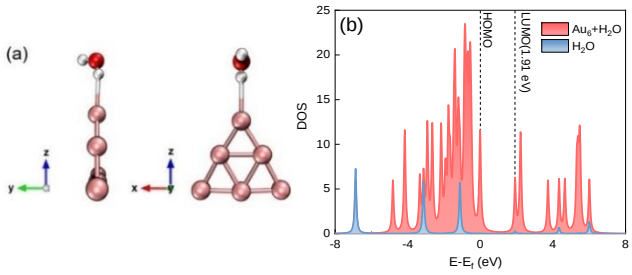

Fig. 1. (a) Front and side view of system of a H_2O molecule adsorbed on the tip of a Au6 cluster. (b) Projected density of states (PDOS) of H_2O and total density of states (DOS) of system.

2.2 Time-dependent density functional theory (TDDFT) and Ehrenfest dynamics simulations

Linear response TDDFT can calculate the excitations by Casida's equations. Optical spectra was obtained by broadening excitations with a 0.0002 a.u. width of the Lorentzian. Ehrenfest dynamics simulations were performed based on the ground state calculation with Approximated Enforced Time-Reversal Symmetry and temperature fluctuated around 300 K. The external electric field of laser was provided as:

$$E(\omega,t) = E_{\max}\exp\left[-\frac{(t-t_0)^2}{2\tau^2}\right]\cos\left[\omega(t-t_0)\right] \quad (1)$$

where ω is the excitation frequency, τ is the width of the laser pulse (set as 1.6 fs), t_0 is the center of the Gaussian pulse (set as 6.6 fs).

3. RESULTS AND DISCUSSION

3.1 Ground State calculation

When adsorbed on the surface of metal nanoparticles, the molecular orbitals of water will be hybridized and energy gap of the frontier orbitals will decrease slightly, from 2.01 eV to 1.91 eV (Figure 1b). To depict electronic structure of the system in detail, ground-state calculation was done after optimization. 11 unoccupied orbitals were used throughout the calculation and wave functions are shown in Figure 2. As illustrated in Figure 2, it can be recognized that the 42nd and 48th molecular orbitals have distinctive features of H_2O antibonding. Adjusting the isosurface value to be smaller, antibonding orbital properties could be also found in the 38th, 39th and 46th orbitals. These molecular orbitals are all the target orbitals for charge transfer. Wave functions of antibonding orbitals can clearly reflect the chemical interface between the metal nanoparticles and adsorbate after hybridization.

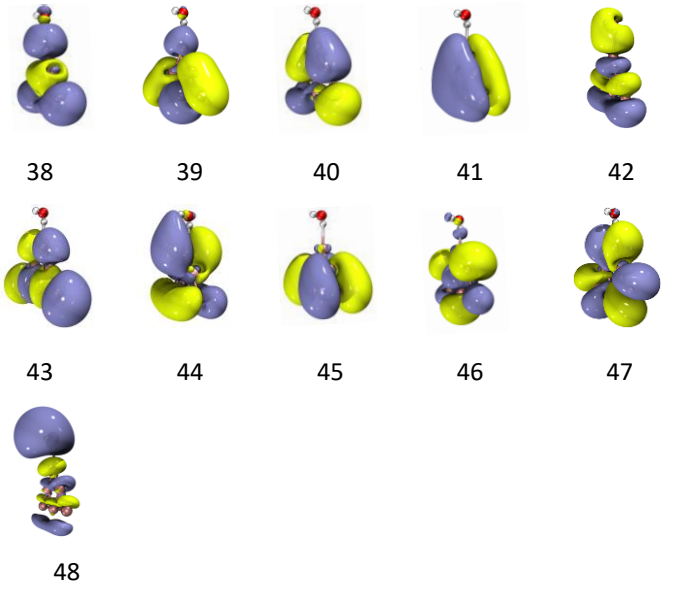

Fig. 2. Wave functions and the corresponding molecular orbital number of the lowest 11 unoccupied Kohn−Sham ortitals (isosurface value is 0.028 e/Å^3).

3.2 Electronic transitions

Absorption spectrum was calculated by the Casida formula of Linear-Response TDDFT. For H_2O@Au6, strong excitations are found at 2.24 eV (f=3.55) and 3.37 eV (f=0.83). Thus, an electric field was set along the z-axis, starting at t=0 fs and fading out after 10 fs by Gaussian wave packet.

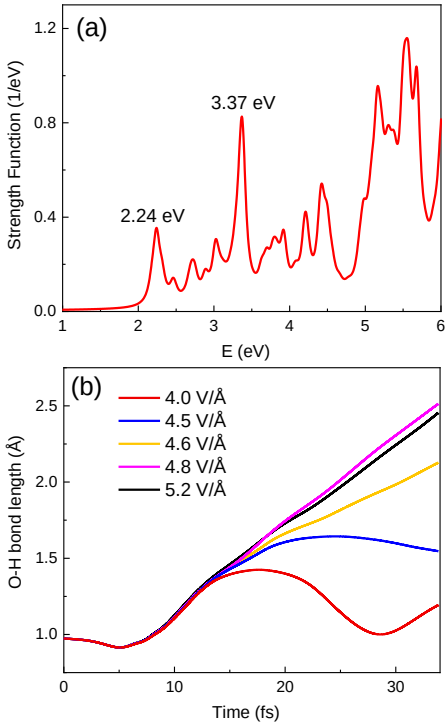

Fig. 3. (a) Oscillator strength functions for H_2O@Au6. (b) Time-dependent evolution of O-H bond lengths at laser frequencies ofA 2.25 eV and different laser intensities E = 4.0, 4.5, 4.6, 4.8, 5.2 V/Å.

At 2.25 eV, O-H bond vibrated within 10 fs, then vibrations slowed down as the laser intensity rising from 4.0 to 4.5 V/Å. When the intensity reached 4.6 V/Å, O-H bond could be up to 2 Å at 30.5 fs and H_2O was decomposed. The more intense the laser, the faster the water broke down, hence there is a critical laser intensity E_c = 4.6 V/Å. It is worth emphasizing that the occurrence of plasmon resonance is frequency dependent, whereas the number of hot electrons gathering around H_2O is determined by the laser intensity, and the critical laser intensity ensures that enough hot electrons are generated to split the water.

For facilitate quantitative observation, O-H bond was supposed to be broken up when the bond length reached 2 Å. The rate of bond breaking was significantly faster at 3.38 eV than at 2.25 eV in Fig. 4. To elucidate the atomic mechanism of water splitting driven by plasmon resonance, further details of charge transfer process were explored from the atomic scale by TDDFT.

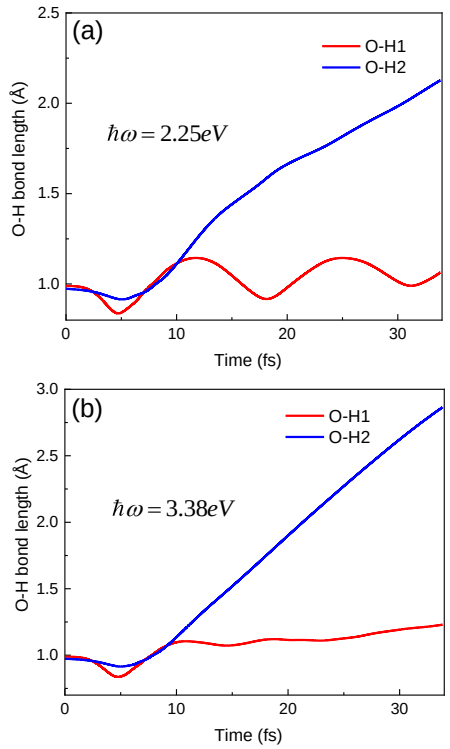

Fig. 4. Time evolution of the two O-H bond length of H2O with Au6 at (a) 2.25 eV and (b) 3.38 eV with intensity of 4.6 V/Å.

As photo-excited at 2.25 eV with intensity of 4.6 V/Å, charges on Au cluster started to transfer to H_2O at 3 fs. The maximum of charge was 10.4 e reached at around 7 fs, after that the charge of H_2O decreased rapidly until it plateaued at around 15 fs. The influence of laser intensity is not significant in this instance. However, when the laser frequency is increased to 3.38 eV, it is significant that more charge was transferred and there was about 13 e around the H_2O at 7 fs.

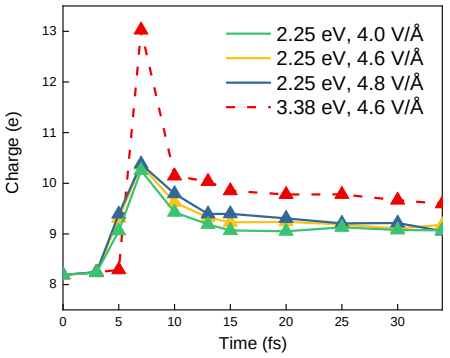

Fig. 5. Time evolution of charge around H_2O at frequencies of 2.25 and 3.38 eV with different laser intensities.

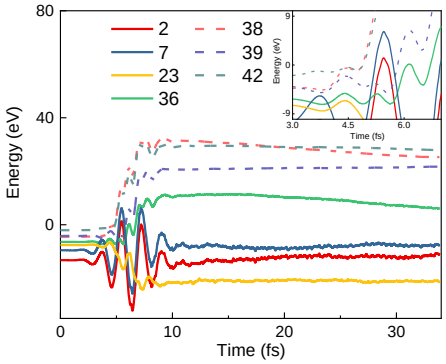

Fig. 6. Time evolution of partial Kohn–Sham orbital energy.

To explain the charge transfer mechanism, time-dependent molecular K-S orbital energies and charge transition coefficients were both calculated and several important eigen states were displayed. Three unoccupied orbitals over the Fermi energy level including LUMO and four occupied orbitals were chosen in Fig. 6. Solid lines indicate partially occupied orbitals, while dashed lines represent unoccupied antibonding orbitals. From 5 to 10 fs, energies of occupied and unoccupied orbitals can be seen to overlap in Fig. 6, where the charge transition happened.

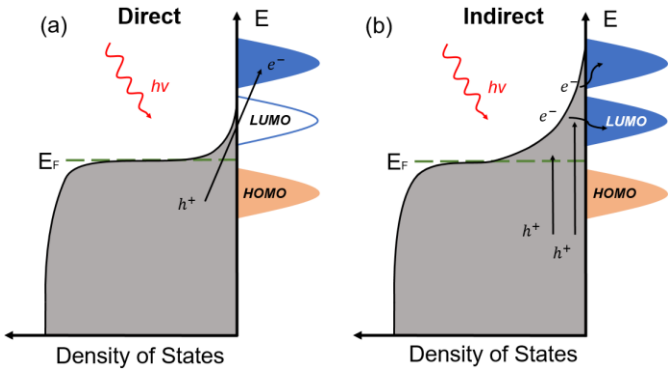

Fig. 7. Charge excitation modes in metals. (a) Direct charge excitation. (b) Indirect charge excitation. Photon absorption produces athermal distributed electron-hole pairs (shaded area) within the metal, and energetic electrons are transferred from the metal into the orbitals of the adsorbent (blue area) during the further cooling.

The main pathways for electron-hole pairs generated during photoexcitation are as follows: (1) Direct, resonant transitions from occupied states to unoccupied states during plasmon decay within the hybrid orbitals, which is called chemical interface damping (CID)[1] as illustrated in Fig. 7a. (2) Indirect transitions from occupied states below the E_F level to unoccupied states above the E_F level within metal and excite hot electrons, which is known as Landau damping[30,31] as illustrated in Fig. 7b.

Ideally, excitation modes of hot-electron can be observed applying a continuous plane-wave laser more

conveniently. Few orbitals that make the dominant contribution to the density change are presented in Fig. 8. Two types of transition can be clearly distinguished. As in Fig. 8a, one is regular high-frequency synchronized oscillations (36 to 38) and the other is smooth amplitude variations (7, 2 to 38). The former is the oscillation that constitutes the plasmon resonance, which implies the direct charge excitation. For smoothly fluctuating transition (2 to 38 in Fig. 8b), it is excitation frequency ω_p that almost equal to the difference between the orbital and the LUMO energy, thus hot-carriers are generated by single-particle excitation within metal and then inject into unoccupied orbits. This type of excitation is classed as indirect charge excitation. Transition along with plasmon resonance dominated for the excitation at 2.25 eV while hot-electrons produced through single-particle excitation dominated at 3.38 eV. Comparing Fig. 8a with 8b, one can see that in exception to the charge oscillations due to plasmon resonance, more hot-electrons are excited through single-particle at 3.38 eV than 2.25 eV.

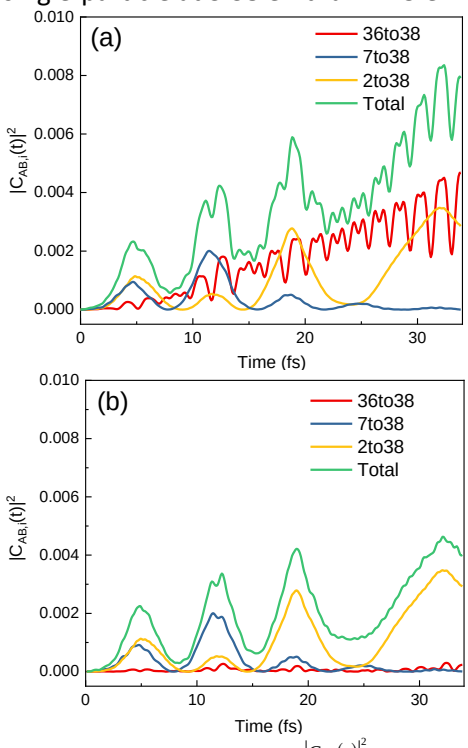

Fig. 8. Charge transition coefficients $|C_{j,i}(t)|^2$ at excitation energies of (a) 2.25 eV and (b) 3.38 eV under a continuous plane-wave laser with an amplitude of 0.01 V/Å.

4. CONCLUSIONS

In summary, DFT, LR-TDDFT and Ehrenfest dynamics simulations were performed to investigate the atomic processes involved in dissociation of H_2O adsorbed on Au6 clusters. This process could be applicable to other plasmonic metal in water splitting, which may have general relevance for plasmon-mediated photocatalysis. Antibonding orbitals of H_2O can be supported by hot electrons from both indirect single-particle excitation and direct plasmon dephasing even the laser faded, inducing the water splitting. As the laser field exists, both plasmon decay and single-particle modes can produce hot electrons simultaneously, however, the main excitation mode differs at different frequencies. The transient energetic electrons generated by dephasing of plasmon are significantly more favorable to the photochemical process, since they can reach higher energy than the excitation energy. Charge transition coefficient analysis allows a fast discrimination between the two hot-electron production pathways at different excitation frequencies. A consideration in combination with excitation frequency, absorption and hot electron production methods is an effective and fast way to screen the favorable microstructures.

ACKNOWLEDGEMENT

This work was supported by the Basic Science Center Program for Ordered Energy Conversion of the National Natural Science Foundation of China (No. 51888103), National Key R&D Program of China (No. 2021YFF0500700), and Natural Science Foundation of Jiangsu Province (BK20200072).

REFERENCE

[1] Kale M J, Avanesian T, Christopher P. Direct Photocatalysis by Plasmonic Nanostructures. ACS Catalysis 2013;4(1):116-128.

[2] Mukherjee S, *et al*. Hot electrons do the impossible: plasmon-induced dissociation of H2 on Au. Nano Lett 2013;13(1):240-7.

[3] Kim Y, Dumett Torres D, Jain P K. Activation Energies of Plasmonic Catalysts. Nano Lett 2016;16(5):3399-407.

[4] Yu X, *et al*. Synergistic Effect Induced High Photo-thermal Performance of Au Nanorod@Cu7S4 Yolk–Shell Nanooctahedron Particles. The Journal of Physical Chemistry C 2016;120(43):24533-24541.

[5] Linic S, Aslam U, Boerigter C, Morabito M. Photochemical transformations on plasmonic metal nanoparticles. Nat Mater 2015;14(6):567-76.

[6] He L, Liu C, Tang J, Zhou Y, Yang H, Liu R, Hu J. Self-catalytic stabilized Ag-Cu nanoparticles with tailored SERS response for plasmonic photocatalysis. Applied Surface Science 2018;434:265-272.

[7] Hartland G V, Besteiro L V, Johns P, Govorov A O. What's so Hot about Electrons in Metal Nanoparticles? ACS Energy Letters 2017;2(7):1641-1653.

[8] Sundararaman R, *et al*. Theoretical predictions for hot-carrier generation from surface plasmon decay. Nature Communications 2014;5(1):5788.
[9] Besteiro L V, *et al*. Understanding Hot-Electron Generation and Plasmon Relaxation in Metal Nanocrystals: Quantum and Classical Mechanisms. ACS Photonics 2017;4(11):2759-2781.
[10] Boerigter C, Aslam U, Linic S. Mechanism of Charge Transfer from Plasmonic Nanostructures to Chemically Attached Materials. ACS Nano 2016;10(6):6108-15.
[11] Rao V G, Aslam U, Linic S. Chemical Requirement for Extracting Energetic Charge Carriers from Plasmonic Metal Nanoparticles to Perform Electron-Transfer Reactions. J Am Chem Soc 2019;141(1):643-647.
[12] Chavez S, Rao V G, Linic S. Unearthing the factors governing site specific rates of electronic excitations in multicomponent plasmonic systems and catalysts. Faraday Discuss 2019;214:441-453.
[13] Boerigter C, Campana R, Morabito M, Linic, S. Evidence and implications of direct charge excitation as the dominant mechanism in plasmon-mediated photocatalysis. Nat Commun 2016;7:10545.
[14] Wu K, *et al*. Efficient hot-electron transfer by a plasmon-induced interfacial charge-transfer transition. Science 2015;349(6248):632-635.
[15] Sivan Y, Un I W, Dubi Y. Assistance of metal nanoparticles in photocatalysis - nothing more than a classical heat source. Faraday Discuss 2019;214:215-233.
[16] Ingram D. B, Linic, S. Water splitting on composite plasmonic-metal/semiconductor photoelectrodes: evidence for selective plasmon-induced formation of charge carriers near the semiconductor surface. J Am Chem Soc 2011;133(14):5202-5.
[17] Foerster B, *et al*. Chemical Interface Damping Depends on Electrons Reaching the Surface. ACS Nano 2017;11(3):2886-2893.
[18] Hernley P A, Linic S. Modeling the Impact of Metallic Plasmonic Resonators on the Solar Conversion Efficiencies of Semiconductor Photoelectrodes: When Does Introducing Buried Plasmonic Nanostructures Make Sense? The Journal of Physical Chemistry C 2018;122(42):24279-24286.
[19] Beck D E. Self-consistent calculation of the eigenfrequencies for the electronic excitations in small jellium spheres. Phys Rev B Condens Matter 1987;35(14):7325-7333.
[20] Puska M J, Nieminen R M, Manninen M. Electronic polarizability of small metal spheres. Phys Rev B Condens Matter 1985;31(6):3486-3495.
[21] Ma J, Wang Z, Wang L W. Interplay between plasmon and single-particle excitations in a metal nanocluster. Nat Commun 2015;6:10107.
[22] Townsend E, Bryant G W. Plasmonic properties of metallic nanoparticles: the effects of size quantization. Nano Lett 2012;12(1):429-34.
[23] Yan L, Wang F, Meng S. Quantum Mode Selectivity of Plasmon-Induced Water Splitting on Gold Nanoparticles. ACS Nano 2016;10(5):5452-8.
[24] Wu Q, *et al*. Mechanistic Insights into Photo-catalyzed H2 Dissociation on Au Clusters. J Am Chem Soc 2020;142(30):13090-13101.
[25] Andrade X, *et al.* Time-dependent density-functional theory in massively parallel computer architectures: the OCTOPUS project. J Phys Condens Matter 2012;24(23):233202.
[26] Castro, *et al*. Octopus: A tool for the application of time-dependent density functional theory. physica status solidi (b) 2006;243:2465–2488.
[27] Humphrey W, Dalke A, Schulten K. VMD: Visual molecular dynamics. Journal of Molecular Graphics 1996;4(1):33-38.
[28] Troullier N, Martins J L. Efficient pseudopotentials for plane-wave calculations. Phys Rev B Condens Matter 1991;43(3):1993-2006.
[29] Idrobo J C, Walkosz W, Yip S F, Öğüt S, Wang J, Jellinek J. Static polarizabilities and optical absorption spectra of gold clusters (Aun,n=2–14 and 20) from first principles. Phys. Rev. B 2007;76(20):5422.
[30] Brongersma M L, Halas N J, Nordlander P. Plasmon-induced hot carrier science and technology. Nat Nanotechnol 2015;10(1):25-34.
[31] Khurgin J B. How to deal with the loss in plasmonics and metamaterials. Nat Nanotechnol 2015;10(1):2-6.